Catalysis Letters Vol. 100, Nos. 3–4, April 2005 (© 2005)
DOI: 10.1007/s10562-004-3450-9

Synthesis and characterisation of highly dispersed Ni/SiO_2 catalysts prepared by gas-phase impregnation/decomposition (GPI/D) of a Ni(II) β-diketonate precursor complex

Lorenzo Stievano[a,*], Nassima Kemache[a], Nassira Chakroune[a,b], and Jean-Françcois Lambert[a]

[a]*Laboratoirie de Réactivité de Surface, UMR CNRS 7609, Université Pierre et Marie Curie, case 178, 4 place Jussieu, 75252 Paris cedex 05, France*
[b]*Institut de Physique et de Chimie des Matériaux de Strasbourg, UMR CNRS 7504, Université Luis Pasteur, 23 rue du Loess, 67034 Strasbourg cedex, France*

Received 9 November 2004; accepted 24 November 2004

Silica-supported nickel catalysts have been prepared by a solventless technique involving the deposition of the $[Ni(tmen)(acac)_2]$ precursor from the gas phase. According to UV–vis and IR spectroscopy and to elemental analysis, the initial deposition step results in the grafting of Ni(II) complexes on silanol groups to give predominantly $[Ni(acac)_2 (\equiv Si\text{-}OH)_2]^0$ monomeric inner-sphere complexes, with elimination of the neutral (tmen) ligands into the gas phase. Subsequent thermal treatments in oxidising atmospheres causes an oxidative decomposition of the (acac) ligands without nickel desorption or coalescence into oxide crystallites. The ensuing coordinatively unsaturated Ni(II) centres are reduced to Ni(0) by flowing hydrogen at low temperatures (300 °C), yielding nanosized Ni particles as evidenced by TEM and O_2 titration. Thus, the gas-phase deposition technique represents an interesting alternative to conventional "wet" deposition procedures since it allows one to obtain well-dispersed supported nickel catalysts by reduction at low-temperatures.

KEY WORDS: Ni/SiO_2 catalysts; gas phase impregnation; precursor complex.

1. Introduction

The design of a supported metal catalyst goes through several unit operations (deposition of the active species precursor, drying, calcination and/or reduction, etc.), all of them potentially contributing to the catalytic properties of the final material. Among the successive preparation steps, transition metal complex (TMC) precursor deposition on the support is crucial to maximise the dispersion of the supported metal. Moreover, this step may also influence the electronic properties and stability of a supported metal, all contributing to the final catalytic performance [1]. Therefore, the ability to understand the interactions between the TMC precursor and the support is of primordial importance to develop an active and stable catalyst.

Classical preparation routes commonly involve the deposition of the TMC from an aqueous solution through either selective adsorption or incipient wetness impregnation. In both methods, the interaction between the TMC and the support is mediated by the solvent, which strongly influences the chemical state of the support surface and the mechanism of TMC adsorption [2]. In some cases, an attractive alternative is to deposit the TMC from the gas phase through the so-called Gas Phase Impregnation-Decomposition (GPI-D) method [3]. In this way, the TMC chemisorbs through a direct surface reaction with adsorption sites of the support, without complications arising from the participation of solvent molecules. GPI-D procedures require of course the use of highly volatile, and therefore non-ionic, TMC precursors; among these, acetylacetonate complexes have often been used.

In the particular case of supported nickel metal catalysts, many synthetic strategies have been employed to maximise the final dispersion of the metal particles and their stability during the catalytic activity. Although supported nickel catalysts prepared from acetylacetonate complexes showed promising properties both in dispersion [3] and in stability during catalysis [4], only a few results have been reported for catalysts prepared from Ni acetylacetonate precursors in solution [4–7], and even less are reported for catalysts prepared by the GPI-D method [8–10].

For Ni/alumina catalysts, the best studied system until now, both preparation procedures seem to lead to a similar adsorbed species. In all cases, it has been suggested that the adsorption of $[Ni(acac)_2]$ occurs through a surface reaction with the loss of one $(acac)^-$ ligand (which either remains bound to the Al^{3+} ions on the surface or is desorbed as Hacac) and the subsequent formation of a surface complex where one or more aluminol (or aluminolate) groups of the support surface form coordinative bonds to the Ni(II) center [6–8, 10, 11]: this is a case of inner-sphere adsorption.

* To whom correspondence should be addressed.
E-mail: stievano@ccr.jussieu.fr

1011-372X/05/0400–0169/0

For the Ni/silica system, on the contrary, the structure of the adsorbed species has not been clarified yet. On the one hand, catalysts prepared by impregnation from THF solutions of $[Ni(acac)_2(H_2O)_2]$ lead to the formation of ill-defined oxide-like nickel species at the surface [5]. This behaviour has been related to the likely instability of the $[Ni(acac)_2(H_2O)_2]$ starting complex, both in the THF solution and after adsorption on the surface [11]. On the other hand, Babich et al. reported, for samples prepared by GPI-D, FT-IR spectra very similar to that of the starting bulk material, $[Ni(acac)_2]$, indicating that the acetylacetonate ligands are still coordinated to nickel atoms in the surface species [8]. In spite of this similarity, the same authors found a Ni:acac molar ratio of about 1:1 for the adsorbed species, suggesting that the Ni atom is coordinated only by one (acac) ligand: therefore, they proposed a tentative tricoordinated surface [(≡SiO)Ni(acac)] species. Such a scheme, although reflecting the experimentally found stoichiometry, leaves the Ni centre strongly uncoordinated [8]. In all Ni/silica catalysts prepared from acetylacetonate precursors, however, the strong reactivity of the surface groups of silica towards the Ni complex precursor leading to the formation of the adsorbed species was emphasized.

An alternative approach for the deposition of well-defined species has recently been applied to the preparation of thin metal films through Metal-Organic Chemical Vapour Deposition (MOCVD) of TMCs [12,13]. In this approach, the precursor complex to be evaporated contains an ancillary Lewis base ligand that allows, on the one hand, the coordinative saturation of the precursor and, on the other hand, is sufficiently labile to be easily exchanged with the surface Lewis-base groups of the substrate or support. An additional interest of this approach is to provide more volatile and stable monomeric precursors [12].

In the present work, a similar approach is employed to prepare Ni/silica catalysts by GPI-D from a well-defined acetylacetonate precursor, $[Ni(tmen)(acac)_2]$ (abbreviated as $NiTA_2$). This complex has long been known, together with several analogues, for its chromotropic properties [13], and its crystal structure has been recently published [14]. $NiTA_2$ is used here to obtain a well-defined Ni^{2+} complex grafted on SiO_2, which is subsequently decomposed to produce highly dispersed Ni metal particles on silica.

2. Experimental

2.1. Materials

Preparation of [Ni(tmen)(acac)$_2$] ($NiTA_2$)

The Ni complex $[Ni(tmen)(acac)_2]$ (tmen = N,N,N′,N′-tetramethylethanediamine, acac = acetylacetonate), hereafter denoted as $NiTA_2$ was prepared following the early method of Fukuda and Sone [15]: 30 mL of a solution containing 10 mmol of tmen, 20 mmol of acetylacetone and 5 mmol of Na_2CO_3 in chloroform are added to an aqueous solution of 10 mmol of $Ni(SO_4) \cdot 6H_2O$. The organic phase, strongly coloured in blue, is then separated and concentrated until the appearance of the green-blue crystals of $NiTA_2$. These crystals can then be further purified by evaporation at 150 °C in an flow of Ar and following recondensation at room temperature.

2.2. Gas-phase impregnation/decomposition (GPI/D) of $NiTA_2$ on silica

In a typical GPI/D experiment, the appropriate amount of $NiTA_2$ to give a total metal loading between 2 and 4 % is placed on the bottom of a glass U-tube reactor fitted with a quartz frit. About 1.5 g of silica (Aerosil 380 from Degussa, BET surface area of 380 ± 20 $m^2\ g^{-1}$ from N_2 physisorption at 77 K), previously dehydrated at 100 °C overnight, are placed on the frit, and the reactor is homogeneously heated to 165 °C for 4 h in argon flow (100 mL min^{-1}), in order to allow the complete evaporation of the starting $NiTA_2$ at the bottom of the U-tube reactor.

The decomposition of the adsorbed $NiTA_2$ species to obtain grafted Ni^{2+} ions on the silica support is obtained by calcination in airflow at 330 °C. This temperature was chosen in accordance with temperature-programmed oxidation experiments (*vide infra*). Finally, reduction of the calcined samples to Ni metal particles dispersed on SiO_2 is carried out in a H_2 flow at 400 °C for 1 h.

2.3. Physico-chemical characterisation

The contents of Ni, C, and N in the supported samples were determined by elemental analysis (Centre d' Analyses du CNRS, Vernaison (France)).

X-ray powder diffraction (XRD) patterns were collected on a Siemens D 500 X-ray diffractometer (Cu K_α, wavelength = 1.5406 Å). The scanning range was set between 5° and 80° (2θ) with a step size of 0.02°.

Differential thermal gravimetry experiments were performed in air or dinitrogen flow (120 mL min^{-1}) with a heating rate of 50 °C min^{-1} on a TG/DTA 220 thermal analyzer (Seiko Instruments Inc.) For each experiment, 6 to 10 mg of sample were used. Before the measurement, the sample was purged in the flow for about 1 h to eliminate most physisorbed water and obtain a stable baseline.

The UV–vis–NIR spectra were recorded on a Cary 5E UV–vis–NIR spectrometer, which permits measurements on solid samples by a diffuse-reflectance light path. The samples were first ground to a fine powder, and subsequently installed into the sample cell (a 5 cm diameter disk) and their surface smoothed. The measurements were carried out in air at room temperature.

FT-IR spectra were recorded in air at room temperature on a Vector 22 Infrared Spectrometer (Bruker). The spectrum of $NiTA_2$ was measured in a KBr pellet with a sample concentration of a few percents by weight. For the silica supported samples, self-supported pellets were employed. FT-IR spectra of the pure tmen and Hacac ligands were measured for comparison purposes.

Quantitative Temperature Programmed Reduction (TPR) profiles were obtained on about 80 mg of sample by using a gas mixture of 5% H_2 in Ar, a gas flow rate of 20 L h^{-1} g^{-1} and a heating rate of 7.5 °C min^{-1}. The H_2 consumption was measured by a differential thermal conductivity detector (TCD) placed after a desiccator aimed at removing the water produced during reduction.

O_2 titration experiments were performed by the dynamic pulse technique on a Micromeritics Pulse Chemisorb 2700 apparatus (50 μl O_2 pulses of in a 15 mL min^{-1} Ar flow) operating at 30 °C. Prior to measurements, the samples were pretreated as follows: reduction in H_2 flow (60 L h^{-1} g^{-1}) at 400 °C for 1 h (heating ramp 10 °C min^{-1}), outgassing in Ar flow (60 L h^{-1} g^{-1}) at 400 °C for 1 h and finally cooling down to 30 °C.

The morphologic characterisation of the supported Ni metal particles was performed in a JEOL 100 CXII Transmission Electron Microscope (TEM) operating at 100 kV. In order to obtain suitable samples, the as-obtained powders were dispersed in ethanol by ultrasonication. A drop of the solution was then deposited onto a thin holey-carbon film supported on a copper microscopy grid (200 mesh, 3.05 mm) and left to dry. The SiO_2 grains, well separated on the thin holey-carbon film, may thus be characterised by TEM. The analysis of the size and distribution of the Ni particles has been performed by TEM imaging. The histograms of metal particle size have been established by counting more than 1000 particles in several different negatives.

3. Results and discussion

3.1. Characterisation and thermal properties of $NiTA_2$

The Ni complex, $NiTA_2$, is green-blue compound with a crystal structure [14] isomorphous to that of the corresponding Co(II) complex, $[Co(acac)_2(tmen)]$ [13]. Both complexes are monomeric and crystallise in the same monoclinic space group (Pl *n*l). In the $NiTA_2$ monomer, tile metal adopts a slightly distorted octahedral NiO_4N_2 coordination (the two nitrogen atoms are constrained to be in a *cis* geometry).

This Ni precursor, $NiTA_2$, was characterised by FT-IR and UV–vis–NIR spectroscopy, whereas its thermal behaviour and stability were investigated by combined DTG and DTA.

The infrared adsorption bands of $NiTA_2$ can be interpreted taking into account its monomeric structure and by comparison to previous studies on similar compounds, such as $[Ni(acac)_2(H_2O)_2]$ [16] or other metal acetylacetonates [17]. On this basis, the FT-IR spectrum of $NiTA_2$ (figure 1) can be divided into three main regions:

1. The first region, between 3200 and 2600 cm^{-1}, contains the C-H stretching vibrations of the several methyl and methylene groups of (acac) and (tmen) ligands.
2. The middle region, between 1800 and 1000 cm^{-1}, which contains the stretching vibration of the C=O and C=C groups, and the bending and rocking modes of the C—H groups.
3. The low-frequency region, between 1000 and 400 cm^{-1}, where the stretching vibration of the C—CH_3 and Ni—O bonds, and the symmetric bending modes of the C—H groups are present.

In particular, the bands at 1609 and 1516 cm^{-1}, assigned to the ν(C=O) and ν(C=C) mixed vibrations of the acetylacetonates, are at the same wavelengths as previously observed for the same compound [15], in agreement with the formation of the proposed structure.

The UV–vis–NIR spectrum of $NiTA_2$ is showed in figure 2. In the near-IR region of the spectrum, three main bands are present: two bands at 1693 and 1736 nm, which can be attributed to the second harmonics of the ν(C—H) vibrations of (tmen) and (acac), and one narrow band at 2258 nm followed by a large adsorption, which is most probably a convolution of combination bands of the type ν(C—H) + δ(H—C—H). In the UV–vis region of the spectrum, four strong adsorption bands are present,

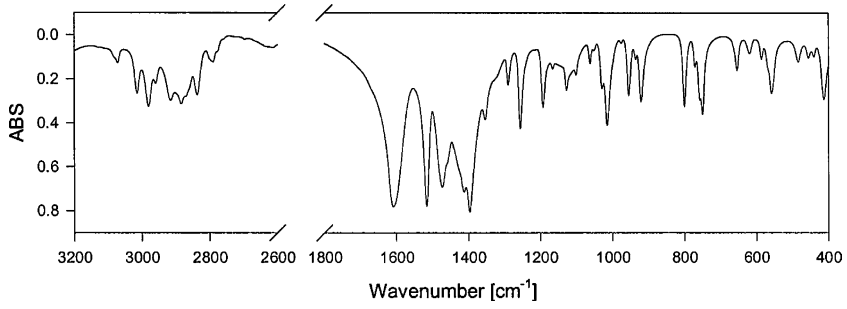

Figure 1. FT-IR spectrum of pure $NiTA_2$.

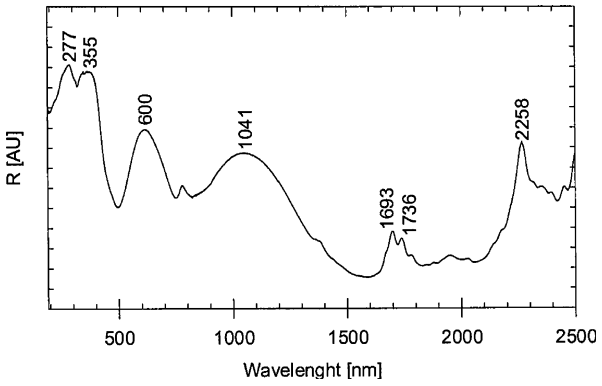

Figure 2. UV–vis–NIR spectrum of pure $NiTA_2$.

agreeing well with an octahedral coordination around the Ni^{2+} centre. In fact, the three bands at 1041, 600 and 355 nm correspond to the three spin-allowed transitions characteristic of Ni^{2+} (d^8) in an octahedral field [18]. The band at 355 is partially superimposed to the charge-transfer adsorption band, which is visible at higher energies (277 nm).

Combined DTG and DTA measurements on $NiTA_2$ in nitrogen flow are shown in figure 3. The DTA endothermic event at 96 °C corresponds to the melting point of $NiTA_2$, in agreement with the results of Saito et al. [19]. The DTG pattern shows that the evaporation of $NiTA_2$ already starts at rather low temperatures, but, under our experimental conditions, becomes significantly high only at about 140 °C. The evaporation of the complex is completed at about 200 °C. Therefore, temperatures in the 140–200 °C range have been considered as the evaporation temperature for the following GPI-D experiments on silica, and, after several preliminary tests, an optimal deposition temperature of 165 °C has been selected.

3.2. Grafting of $NiTA_2$ on SiO_2

Sample $NiTA_2/SiO_2$ was obtained by vaporisation of the neutral [Ni(acac)$_2$(tmen)] at 165 °C in an argon flow and subsequent deposition, at the same temperature, on non-porous silica. The X-ray diffractogram of this material (not shown) only exhibits the, broad pattern of amorphous silica with no contribution from crystalline $NiTA_2$, indicating that the initial complex is not adsorbed in the crystalline form but is rather dispersed on the surface of silica.

Elemental analysis data are shown in Table 1. The total amount of nickel deposited on this sample from the gas phase is about 3%. Moreover, the measured C/Ni and N/Ni molar ratios of about 9 and 0.8, respectively, are significantly different from the values of 16 and 2, which would be expected if the $NiTA_2$ complex were deposited intact on the surface of silica. The very low value of the N/Ni ratio, together with a value of C/Ni of about 10, rather suggests that the (tmen) ligand is lost during the surface reaction with the silica surface, and that the Ni centre remains adsorbed on SiO_2 surrounded only with the two (acac) ligands.

The structure of the adsorbed Ni complex can be inferred by the combined analysis of FT-IR and UV–vis spectra. In fact, the UV–vis spectrum of $NiTA_2/SiO_2$ is different from that of the starting bulk $NiTA_2$ (figure 4).

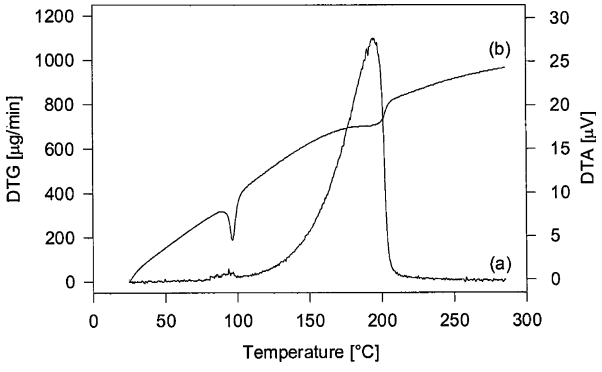

Figure 3. DTG (a) and DTA (b) pattern under nitrogen of pure $NiTA_2$.

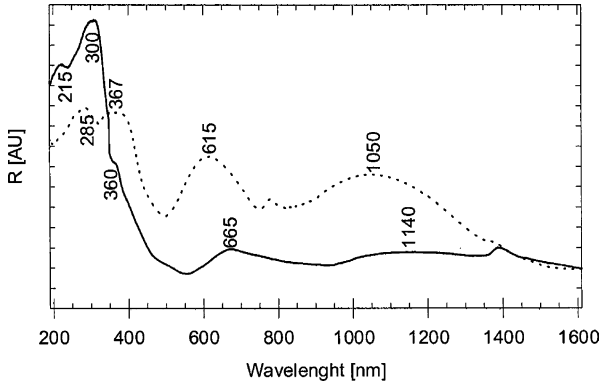

Figure 4. UV–vis spectrum of $NiTA_2/SiO_2$ (filled line). The spectrum of pure $NiTA_2$ (dotted line) is shown for comparison purposes.

Table 1
Elemental analysis of the supported samples $NiTA_2/SiO_2$ and Ni^{2+}/SiO_2. The theoretical values for pure $NiTA_2$ are shown for comparison purposes

Sample	Ni [wt%]	C [wt%]	N [wt%]	C/Ni molar ratio	N/Ni molar ratio	CN molar ratio
$NiTA_2$ (theoretical)	15.7	51.5	7.5	16	2	8
$NiTA_2$	14.4	48.8	7.2	16.5	2.1	7.9
$NiTA_2/SiO_2$	2.8	5.3	0.6	9.1	0.8	11.0
Ni^{2+} /SiO2	3.0	1.3	> 0.10	2.1	> 0.1	–

The weakening and the bathochromic shift of the three main bands typical of Ni^{2+} (d^8) in an octahedral field together with the relative increase in intensity of the charge transfer band at 300 mm all agree with a modification of the coordination sphere at the Ni centre. In this case the d–d adsorption band in the 300–400 nm region, superimposed to the large tail of the charge-transfer band of the spectrum determines the yellow colour of the adsorbed Ni complex. A similar spectral behaviour was attributed by Rossman et al. [20] to the presence of a distorted octahedral coordination of the Ni^{2+} centre in solid Ni oxides solutions, such as $MgSiO_3$:Ni. As regards the bathochromic shift of the d–d bands, it can be assigned to the substitution of the N-containing (tmen) ligands by lower crystal field ligands such as surface silanol/silanolate groups [2l].

Due to the superposition of the intense bands of the silica support, the FT-IR spectrum of $NiTA_2/SiO_2$ can only be exploited above 1250 cm^{-1}. The infrared adsorption spectrum of sample $NiTA_2/SiO_2$ in the 1700–1300 cm^{-1} range (Fig. 5) is remarkably different from that of pure $NiTA_2$. The bands between 1700 and 1500 cm^{-1}, attributed to the ν(C═O) and ν(C═C) vibrations, are in fact subjected to marked shifts, indicating an increase of the bond strength between the (acac) ligands and the Ni^{2+} cation. At the same time, the band at 1473 cm^{-1}, attributed to the δ(CH3) vibrations of the (tmen) ligand, strongly decreases in intensity. In short, the spectrum on the adsorbed Ni species becomes very similar to that observed for $[Ni(acac)_2]$, pure or adsorbed on silica [6–8]. Moreover, the absence of bands at 1730 and 1710 cm^{-1}, typical of pure Hacac, indicate that all (acac-) groups on the sample are bound to Ni centres.

These results concordantly substantiate the formation of a well-defined specific $[Ni(acac)_2S_2]$ surface complex, with the exchange of the (tmen) ligand with two silanol and/or silanolate groups (S) on the surface of the silica. To quote only one closely related example, upon aqueous deposition of $[Ni(en)_2(H_2O)_2]^{2+}$ on silica [21], the Ni complex exchanges its two aqua ligands with two support silanol/silanolate groups and forms an octahedral inner-sphere grafted complex, which may be either the positively charged $[Ni(en)_2(\equiv Si–OH)_2]^{2+}$ or the neutral $[Ni(en)_2(\equiv Si–O)_2]$, depending upon the electrical charge of the support surface.

In the case of $NiTA_2$ deposited from the gas phase, the surface of the silica is not expected to be ionised, and the surface complex would be $[Ni(acac)_2(\equiv Si–OH)_2]^0$, i.e., formed with two silanols rather than with two silanolate groups. The neutral (tmen) ligand is probably eliminated in the gas phase, although the presence of a small residual quantity of nitrogen in chemical analyses suggests that a minor part of it might still be adsorbed on the surface of silica.

This hypothesis agrees well with the DTG analysis of $NiTA_2/SiO_2$ in airflow, reported in figure 6. Together with the desorption of water at low temperature, two superimposed weight losses, centred at 250–310 °C, are present in the DTG pattern, the second and sharper one being associated with an exothermic effect in the DTA pattern (not shown). The integration of both signals, after subtracting the contribution of water desorption, gives a relative weight loss of 7.50%, which, considering the molar ratio of the different species and a Ni loading of 3%, would correspond to the loss of 1.7 molecules of (acac) per Ni atom.

Thus, based on UV–vis spectra and other evidence, we suggest the formation of an octahedral six-fold coordinated Ni^{2+} surface complex upon deposition on silica. Even though different models have been proposed by other authors for the species adsorbed from $[Ni(acac)_2]$ precursors on alumina or on silica [6–8, 10], our hypothesis is quite reasonable if one considers the coordination chemistry of Ni^{2+} with (acac) ligands [22]. For instance, it has long been known that the molecular structure of $[Ni(acac)_2]$ contains polymerised $\{Ni(acac)_2\}_3$ units arranged in such a way that the Ni^{2+} is always hexacoordinated, with six oxygen atoms in bridging positions [23]. Early studies on the coordina-

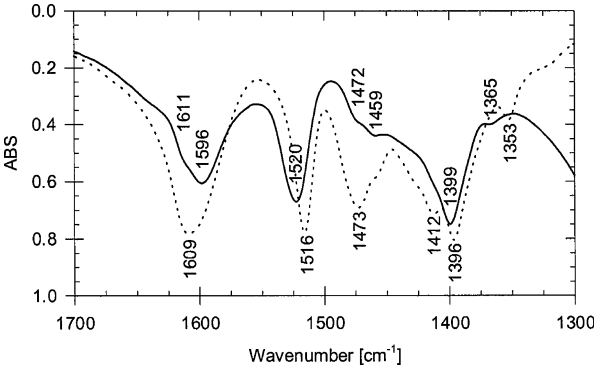

Figure 5. FT-IR spectrum of $NiTA_2/SiO_2$ (filled line) in the range 1700–1300 cm^{-1}. The spectrum of pure $NiTA_2$ (dotted line) is shown for comparison purposes.

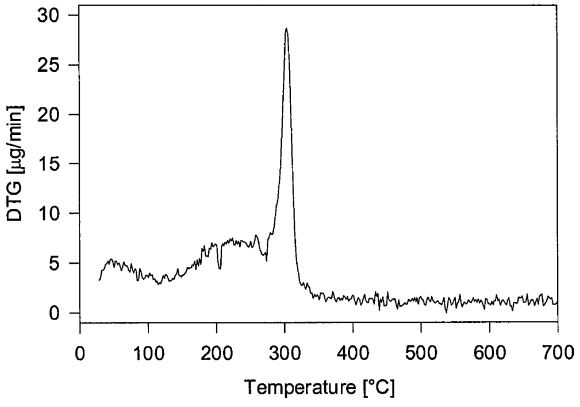

Figure 6. DTG pattern under airflow of the supported $NiTA_2/SiO_2$.

tion on Ni^{2+} with substituted acetylacetonates in different solvents have shown that, when the ligands sterically allow it, the Ni^{2+} centre tends to become six-coordinated either by addition of solvent molecules or other Lewis bases, or by forming polymeric species [24, 25]. In fact, four-coordinated (planar) Ni^{2+} β-ketoenolate are obtained only with bulky substituents on the ketoenolate chain or, for $[Ni(acac)_2]$, in the gas phase, [25].

Slight deviations from the ideal $[Ni(acac)_2(\equiv Si–OH)_2]$ stoichiometry- are detected both in the elemental and in the quantitative DTG analysis of the adsorbed species. In particular, the amount of (acac-) measured after deposition (both by elemental analysis and TGA) is slightly smaller than the expected value. Such an observation might be explained through the formation of a minor fraction of polymeric surface Ni-acac species containing bridging (acac) ligands. These species, which would account for the missing of a small amount of (acac) ligands, would be in line with the previously mentioned tendency of metal acetylacetonates to form polymeric species [24, 25].

Finally, one should note that the anionic ($acac^-$) ligands that compensated the positive charge of the Ni^{2+} centres are eliminated by calcination. Therefore, their charge must be neutralised in some way in the thermal decomposition mechanism; alternatively, the positive charge of the Ni^{2+} must be compensated by a different partner after ligand decomposition, the only reasonable alternative being the silanolate groups.

To summarise, the global complex reaction could be written as two successive steps, as suggested by the two superimposed peaks present in the DTG pattern:

1. $[Ni(acac)_2(\equiv Si–OH)_2]^0 \rightarrow [Ni(acac)(\equiv Si–OH)(\equiv Si–O)]^0 + Hacac_{gas}$(non-oxidative)
2. $[Ni(acac)(\equiv –Si–OH)(\equiv Si–O)]^0 + XO_2 \rightarrow [Ni(\equiv Si–O)_2]^0$ + [oxidative decomposition products]

3.3. *Reactivity of the grafted Ni species and formation of highly dispersed Ni metal particles*

As already stated, the TG analysis shows that decomposition of the grafted Ni complex occurs from about 200 to 320 °C (figure 6). No further weight losses are observed at temperature higher than 330 °C, showing that the oxidation of the grafted precursor is completed at this temperature. For this reason, calcination of the adsorbed complex was performed at 330 °C in order to eliminate the organic ligands and obtain well-dispersed supported Ni^{2+} species.

Elemental analysis after calcination in air at 330 °C (table 1) indicate a Ni loading of 3.0%, which is virtually the, same loading as in initial sample before oxidation. This shows that the grafted complex is not desorbed in the gas phase, as one might have expected considering the high volatility of acetylacetonates.

The models we have proposed so far would imply a high homogeneity of the supported Ni(II) species after calcination in air at 330 °C, as they would consist in coordinatively unsaturated Ni^{2+} grafted on two silanolate groups. This conclusion is substantiated by the ensuing temperature-programmed reduction (TPR) experiments (figure 7). In fact the TPR pattern shows a single-step reduction of the Ni species centred at 340 °C. Quantitative evaluation of the hydrogen consumption gives a H:Ni molar ratio of 2.05, compatible with the reduction of the totality of Ni species from (+II) to 0.

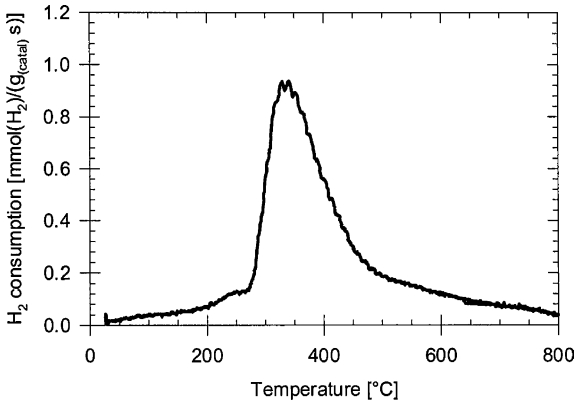

Figure 7. TPR pattern of the calcined Ni^{2+}/SiO_2 species.

In order to evaluate the degree of reduction and the accessibility of the Ni species, the catalysts reduced at 300 °C were titrated with molecular oxygen near room temperature. Oxygen is supposed to react with the surface Ni metal atoms to form a passivating layer on the surface of the metal particles. By assuming that only the first layer of the Ni atoms reacts with O_2 molecules at this low temperature, one can roughly evaluate the dispersion of the Ni particles. If we accept a titration stoichiometry of one oxygen atom per nickel surface atom ($O/Ni_s = 1$), and using the calculation method for metal dispersion, surface area and average crystallite diameter detailed in reference [26], we obtain a high metal dispersion of 65%, corresponding to an average metal particle size of 1.5 nm.

This very high dispersion agrees well with the TEM analysis of the reduced samples. In fact, only small metal particles are visible, evenly spread on the support, whereas no big or agglomerated particles are present. The results of TEM analysis, summarised in the histogram shown in figure 8, give an average particle size of 1.8 nm. Considering that in general only particles larger than about 1.5 nm produce sufficient contrast to be clearly visible in the TEM micrographs, this value is in good agreement with the O_2 titration results. Such well-dispersed metal particles are much smaller than. those obtained by Deposition-Precipitation from aqueous solution, even in favourable cases [27].

With respect to Ni/SiO_2 catalysts prepared through other wet preparation methods, it is interesting to underline that this high dispersion was obtained at a

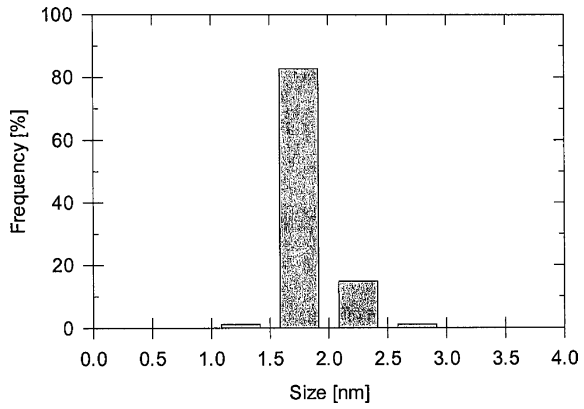

Figure 8. Histogram of the Ni particle size determined by TEM.

rather low reduction temperature. It is usually accepted in the literature that the size of the nickel metal particles in Ni/SiO_2 systems prepared via aqueous precursor species is inversely proportional to the reducibility of the Ni species, i.e., the lower the reducibility (the higher the reduction temperature), the higher the resulting dispersion of the reduced Ni particles [27, 28]. This notion is founded on a reducing mechanism that considers the presence, on the surface of silica, of two different Ni species: nickel oxide (NiO) and surface Ni phyllosilicates. On the one hand, large particles of NiO are reduced by H_2 at a rather low temperature (about 300 °C) through a (nucleation + fast propagation) mechanism producing large metal particles. On the other hand, surface Ni phyllosilicates are stable and strongly bound to the support, and are thus reduced through a rather complicated mechanism at much higher temperatures (about 600 °C). In the latter case, given the low mobility of the Ni species during the propagation step, highly dispersed Ni metal particles are produced.

It is important to notice, however, that these mechanisms are all observed for catalysts prepared via wet deposition procedures. In aqueous solution, silica is expected to partially dissolve at the surface. The silicic acid monomers released in solution can react with the Ni complex precursors in solution via a heterocondensation reaction to form the precipitated Ni phyllosilicate surface species [27]. In contrast, these precipitation steps cannot occur in samples prepared via our GPI-D dry method, and the resulting supported Ni species are different from those usually observed in catalysts prepared through a more classical method.

Therefore, the rather low reduction temperature and the total absence of reduction peaks at temperatures higher than 500 °C both indicate that no bulk Ni silicate species are present. Moreover, the high final dispersion is not compatible with the presence of large NiO particles after the calcination step at 340 °C. On the contrary, these results agree well with the presence of well-dispersed Ni^{2+} species at the surface of silica, obtained by the removal of the ligands through calcination, which are then easily reduced in H_2 flow forming small Ni particles.

Conclusions

$NiTA_2$ has been shown to be an excellent candidate precursor to obtain highly dispersed Ni metal particles on silica by GPI-D. The spectroscopic data evidence the surface reaction of the starting complex with silica, which goes through the exchange of the ancillary (tmen) ligand for surface adsorption sites to form a well-defined inner-sphere grafted Ni complex species. This surface complex can be further decomposed in oxygen flow prior to reduction under mild conditions to obtain highly dispersed Ni metal particles. GPI-D appears as an attractive method for grafting such an active transition metal complex on oxide supports, while avoiding the complications arising from classical methods due to the presence of solvent molecules.

Acknowledgments

The authors gratefully thank Mrs. F. Warmont of the Electron Microscopy Service (UFR Chimie – Université Pierre et Marie Curie) for the microscopic analysis of the samples and Mr. C. de la Porte des Vaux for valuable technical help.

References

[1] J.-F. Lambert and M. Che, J. Mol. Catal. A: Chem. 162(5–18) (2000) 162, 5.
[2] S. Boujday, J.-F. Lambert and M. Che, Topics Catal. 24 (2003) 37.
[3] P. Serp, P. Kalck and R. Feurer, Chem. Rev. 102 (2002) 3085.
[4] N.N. Nichio, M.L. Casella, E.N. Ponzi and O.A. Ferretti, Thermochim. Acta 400 (2003) 101.
[5] J.A.R. Veen, P.C. De Jong-Versloot, G.M.M. Kessel and F.J. Fels, Thermochim. Acta 152 (1989) 359.
[6] R. Molina, M.A. Centeno and G. Poncelet, J. Phys. Chem. B 103 (1999) 6036.
[7] R. Molina, M.A. Centeno and G. Poncelet, J. Phys. Chem. B 103 (1999) 11290.
[8] I.V. Babich, Yu.V. Pluyto, A.D. Van Langeveld and J.A. Moulijn, Appl. Surf. Sci. 115 (1997) 267.
[9] J.-P. Jacobs, L.P. Lindfors, J.G.H. Reintjes, O. Jylha and H.H. Brongersma, Catal. Lett. 25 (1994) 315.
[10] M. Lindblad, L.P. Lindfors and T. Suntola, Catal. Lett. 27 (1994) 323.
[11] P. Voort, M.B. Mitchell, E.F. Vansant and M.G. White, Interface Sci. 5 (1997) 169.
[12] J.R. Babcock, D.D. Benson, A. Wang, N.L. Edleman, J.A. Belot, M.V. Metz and T.J. Marks, Chem. vap. Depos. 6 (2000) 180.
[13] S. Pasko, L.G. Hubert-Pfalzgraf, A. Abrutis and J. Vaissermann, *Polyhedron* 23 (2004) 735; W. Linert, Y. Fukuda and A. Camard, *Coord. Chem. Rev.* 218 (2001) 113.
[14] A. Zeller, E. Herdtweck and Th. Strassner, Coord. Chem. Commun. 7 (2004) 296.
[15] Y. Fukuda and K. Sone, J. Inorg. Nucl. Chem. 34 (1972) 2315.
[16] A.M.A. Bennett, G.A. Foulds and D.A. Thornton, Polyhedron 8 (1989) 2305.

[17] I. Diaz-Acosta, J. Baker, W. Cordes and P. Pulay, J. Phys. Chem. A 105 (2001) 238–244.
[18] F.A. Cotton and G. Wilkinson, in: *Advanced Inorganic Chemistry* (Wiley Interscience, New York, 1962) p. 738.
[19] Y. Saito, T. Takeuchi, Y. Fukuda and K. Sone, Bull. Chem. Soc. Jpn. 54 (1981) 196.
[20] G.R. Rossman, R.D. Shannon and R.K. Waring, J. Solid State Chem. 39 (1981) 277.
[21] J.-F. Lambert, M. Hoogland and M. Che, J. Phys. Chem. B 101 (1997) 10347.
[22] D.P. Graddon, Coord. Chem. Rev. 4 (1969) 1.
[23] G.J. Bullen, R. Mason and P. Pauling, Inorg. Chem. 4 (1965) 456.
[24] J.P. Fackler Jr., Progr. Inorg. Chem. 7 (1966) 361.
[25] J.P. Fackler Jr, M.L. Mittleman, H. Weigold and G.M. Barrow, J. Phys. Chem. 13 (1968) 4631.
[26] C.H. Bartholomew and R.B. Pannell, J. Catal. 65 (1980) 390.
[27] P. Burattin, M. Che and C. Louis, J. Phys. Chem. B 104 (2000) 10482.
[28] P. Burattin, M. Che and C. Louis, J. Phys. Chem. B 103 (1999) 6171.